Electric Power Systems Research 202 (2022) 107573

Contents lists available at ScienceDirect

Electric Power Systems Research

journal homepage: www.elsevier.com/locate/epsr

Reliability modelling of capacitor voltage transformer using proposed Markov model

Omid Haghgoo, Yaser Damchi *

Faculty of Electrical Engineering, Shahrood University of Technology, Shahrood, Iran

ARTICLE INFO

Keywords:
Capacitor voltage transformer
Reliability
Markov model

ABSTRACT

Capacitor voltage transformer (CVT) is one of the most important instrument transformers widely used to prepare the voltage signal for control and protection equipment. The measuring accuracy of CVT plays an important role in the proper operation of the protection system. Therefore, maintaining the accuracy of CVT throughout its lifetime at the desired level is of great significance, and proper maintenance activities must be implemented regarding the equipment conditions. Evaluating the reliability of the CVT over its lifetime is necessary to determine the proper maintenance. Until now, no proper model has been suggested to evaluate the reliability of CVT. Therefore, this paper proposes a new Markov model to evaluate the reliability of CVT. To obtain the model, initially, a Markov model is presented for each subsystem of CVT including capacitor voltage divider (CVD), electromagnetic unit (EMU), and high voltage bushing. Then, by integrating these models, a 10-state extended Markov model is proposed for CVT. Finally, by combining similar states, a 3-state model including healthy, low-quality and failure states is obtained. The simulation results show that the second capacitive group in the CVD subsystem, and the compensating reactor in the EMU subsystem play a major role in the CVT performance.

1. Introduction

With the increasing expansion of power systems, improving the stability and enhancing the reliability of the systems become particularly important. One of the appropriate solutions to maintain the reliability of the power system at the desired level is to improve the performance of the protection system. The input signal of the protection relays is provided by the instrument transformers to perform the protection functions as the favorable or unfavorable operation of the relays depends on these signals. From this perspective, instrument transformers plays a vital role in maintaining the performance of the protection system at the desired level. Capacitor voltage transformers are an example of such instrument transformers used in medium and high voltage networks. Therefore, maintaining the accuracy of this equipment at an acceptable level throughout their lifetime is of great importance. For this reason, the reliability of the CVT must be carefully evaluated in order to provide proper maintenance activities throughout its lifetime.

In general, both simulation and analytical methods can be used to assess the reliability of such equipment. The simulation method is used to predict the system behavior pattern over a period of time, and the Monte Carlo simulation method is one of the most popular methods in this regard. The analytical methods such as the Events tree, Faults tree and Markov process are based on mathematical rules, and problem solving [1-22].

In [1], the reliability of AC / UHVDC systems has been evaluated using Monte Carlo simulation method. In this method, the accuracy of the input information is critical in order to obtain the proper and quality response. In [2], Fuzzy-set logic has been used to improve the analytical method of the Events tree in assessing the reliability of complex issues involving protection systems. In [3], the reliability of engines used in electric vehicles has been evaluated using the analytical method of the Faults tree. In [4], a model for lithium-ion battery has been proposed by composite equivalent modeling.

To evaluate the reliability using the Markov model, initially, the components of the equipment and its various operational states must be identified, and then, the appropriate model must be proposed regarding the identified states.

In [5], a 9-state Markov model has been used to evaluate the reliability of a protection system without considering self-checking and monitoring tests. In [6], the 17-state Markov model has been used to evaluate the reliability and determine the optimum routine and self-checking test time intervals of transmission line protection relays by

* Corresponding author.
E-mail address: damchi@shahroodut.ac.ir (Y. Damchi).

https://doi.org/10.1016/j.epsr.2021.107573
Received 29 December 2020; Received in revised form 11 August 2021; Accepted 5 September 2021
Available online 17 September 2021

Nomenclature

λ_{C1} and λ_{C2} Failure rates of high voltage and medium voltage capacitor, respectively, when CVD subsystem moves from healthy state to failure state.
λ_{1C1} and λ_{1C2} Failure rates of high voltage and medium voltage capacitor respectively, when CVD subsystem moves from healthy state to low-quality state.
λ_{2C1} and λ_{2C2} Failure rates of high voltage and medium voltage capacitor respectively, when CVD subsystem moves from low-quality state to failure state.
λ_{CVD} Equivalent failure rate of CVD subsystem that it moves from healthy state to failure state.
λ_{1CVD} Equivalent failure rate of CVD subsystem that it moves from healthy state to low-quality state.
λ_{2CVD} Equivalent failure rate of CVD subsystem that it moves from low-quality state to failure state.
λ_{Oil} Failure rate of dielectric fluid in CVD subsystem.
λ_{Core} Failure rate of the core.
λ_{W} Failure rate of winding.
λ_{OWD} Equivalent failure rate of dielectric fluid, winding and core in EMU subsystem.
λ_{CR} Failure rate of compensating reactor when it moves from healthy state to failure state in EMU subsystem.
λ_{1CR} Failure rate of compensating reactor that it moves from healthy state to low-quality state in EMU subsystem.
λ_{2CR} Failure rate of compensating reactor that it moves from low-quality state to failure state in EMU subsystem.
λ_{D} Failure rate of damper.
λ_{EMU} Equivalent failure rate of EMU subsystem that it moves from healthy state to failure state.
λ_{1EMU} Equivalent failure rate of EMU subsystem that it moves from healthy state to low-quality state.
λ_{2EMU} Equivalent failure rate of EMU subsystem that it moves from low-quality state to failure state.
λ_{B} Failure rate of high voltage bushing.
λ_{CVT} Equivalent failure rate of CVT that it moves from healthy state to failure state.
λ_{1CVT} Equivalent failure rate of CVT that it moves from healthy state to low-quality state.
λ_{2CVT} Equivalent failure rate of CVT that it moves from low-quality state to failure state.
μ_{C1} and μ_{C2} Repair rates of high voltage and medium voltage capacitor, respectively.
μ_{CVD} Equivalent repair rate of CVD subsystem.
μ_{Oil} Repair rate of dielectric fluid in CVD subsystem.
μ_{Core} Repair rate of the core.
μ_{W} Repair rate of winding.
μ_{OWD} Repair rate of dielectric fluid, winding and core in EMU subsystem.
μ_{CR} Repair rate of compensating reactor.
μ_{D} Repair rate of damper.
μ_{EMU} Equivalent repair rate of EMU subsystem.
μ_{B} Repair rate of high voltage bushing.
μ_{CVT} Equivalent repair rate of CVT.
f_{ij} Transition frequency from i state to j state.

considering self-checking and monitoring tests for relays. In [7], using the 13-state Markov model, has evaluated the reliability and determined the time of periodic test of the transmission line protection system, considering the possibility of failure for the backup protection system. In [8], considering the probability of failure for the backup protection system, the optimum routine and self-checking test time intervals of the protection system has been determined using a 21-state Markov model. In [9], the reliability of the protection system has been evaluated using a 17-state Markov model. In this reference, the effect of the backup protection system performance on the reliability of the transmission line protection system and the time interval of its periodic tests have been investigated. In [10], the reliability of the high voltage circuit breaker has been evaluated using the 6-state Markov model. In [11], the Markov model has been used to evaluate the reliability of the hybrid DC circuit breaker. In [12], a Markov model has been used for the reliability analysis of the power system by considering the failures of the protection system. In this model, the operational modes of the protection system have been divided into 3 stages including the healthy mode, internal failure mode, and external failure mode. In [13], a Markov model has been used to determine the optimal inspection rate of circuit breakers. In [14], the reliability of overcurrent relays has been evaluated using the 32-state Markov model. In [15], the Markov model has been used to evaluate the reliability of an oil nature and air nature (ONAN) power transformer. In this reference, first, the power transformer has been divided into two subsystems in which the winding, core, fluid and fluid tank have been considered as internal components of the power transformer in the first subsystem, and external components including tap-changer and bushings as the second subsystem. Then, by integrating the Markov model of these two subsystems, a final 5-state Markov model has been obtained to evaluate the reliability of the power transformer. In [16], the 11-state Markov model has been used to evaluate the reliability of oil nature and air forced (ONAF) power transformers. In this reference, the power transformer has been divided into three subsystems. The first and second subsystems are the same as the previous reference. The third subsystem involves fans. A Markov model has been presented for each subsystem and finally, by integrating the obtained Markov models, the reliability of the ONAF power transformer has been analyzed. In [17], the Markov model has been used to evaluate the reliability of the static variable reactor (SVC). In this study, only two healthy and faulty states have been considered for the reactor components. In [18], the Markov model has been used to model the lifetime of generator components. Then, a maintenance model has been presented based on the reliability for generators. In [19], the reliability of the magnetically controlled reactor has been evaluated using the Markov model considering the half-capacity state for the winding. In this reference, the effect of heat on the reactor, and then, the effect of this factor on the reliability of the reactor has been investigated. In [20], the reliability evaluation of distribution systems has been carried out by considering parallel capacitors using a 4-state Markov model. In [21], a 17-state Markov model has been proposed to investigate the effect of human error on the failure rate of the transmission line protection system and the optimum routine test time intervals of the system. In the [22], a model for repair and maintenance of CVT has been proposed according to its reliability considering the experiences of the maintenance team.

According to reviewed papers, no model has been proposed yet to evaluate the reliability of CVT that plays an important role in the quality of performance of protection relays. Therefore, in this paper, a 10-state Markov model is proposed to evaluate the reliability of this equipment in order to make appropriate decisions for maintenance activities.

In this regard, first, the different components of the capacitor voltage transformer are identified and then categorized in 3 subsystems. The CVD subsystem, as the first subsystem includes the first and second capacitor groups as well as the dielectric fluid used in this subsystem. The EMU subsystem as the second subsystem includes inductive transformer, damper, compensating reactor and dielectric fluid. High voltage bushing is located in the third subsystem. In order to obtain the CVT Markov model, initially, a 10-state Markov model for the first subsystem, a 9-state model for the second subsystem, and a 2-state model for the high voltage bushing are proposed. Finally, by combining the proposed Markov models, a 10-state model for evaluating the reliability of a capacitive voltage transformer is presented. The results of numerical studies demonstrate that the damper has the greatest impact on the low-quality state of CVT. Moreover, the second capacitive group in the CVD subsystem along with the compensating reactor (CR) in the EMU subsystem, play a major role in the CVT performance. Comparing the obtained results with the presented practical results in [23] verifies the quality of the proposed model.

The rest of this paper is organized as follows. In Section 2, the operation of the various subsystems of CVT is briefly introduced. In Section 3, a new reliability model based on the Markov chain method is proposed to evaluate the reliability of the CVT. Section 4 presents the results of simulation and sensitivity analysis. Finally, the conclusion is presented in Section 5.

2. Capacitor voltage transformer

Due to the low cost and easy installation of CVT compared to inductive voltage transformer at medium and high voltage levels, this type of transformer is widely used for measurement and protection applications in the power network [24]. CVT converts the network voltage to the appropriate voltage for measurement, control and protection systems. In order to have proper operation of the protection systems, the measurement of the voltage in the secondary of the CVT must be performed with acceptable accuracy. Therefore, monitoring the condition of a CVT during its lifetime is of great significance. To monitor the conditions of this equipment, it is important to provide a suitable model to evaluate its reliability.

In order to achieve a suitable model, the structure of the CVT must be carefully examined. Fig. 1 illustrates the circuit structure of a CVT, which generally consists of two subsystems as CVD and EMU. In this study, the CVD consists of two groups of capacitors C1 and C2 and the dielectric liquid which is oil. Capacitor groups are used to reduce high and medium voltages to an acceptable level, for example around 22Kv.

These capacitor groups are designed from several series capacitors according to the type of CVT application at different voltage levels. It is notable that based on the design of the manufacturer, CVT can be composed of one or more capacitor groups that are located on the top part of the CVT and on the top of each other [25]. C1 is known as a high voltage capacitor due to its connection to the CVT voltage input. After reducing the voltage in the first capacitor group, there is a second capacitor group called C2. The conversion ratio of these two capacitor groups provides the appropriate voltage for the middle transformer.

Next to the CVD subsystem is the EMU subsystem. In general, the EMU subsystem consists of a compensating reactor, an inductive transformer, a damper and dielectric fluid. The compensating reactor, which is to compensate for the capacitor effects and phase angle changes caused by the reactance of the CVD, is located in series between the capacitor divider subsystem and the inductive transformer [25].

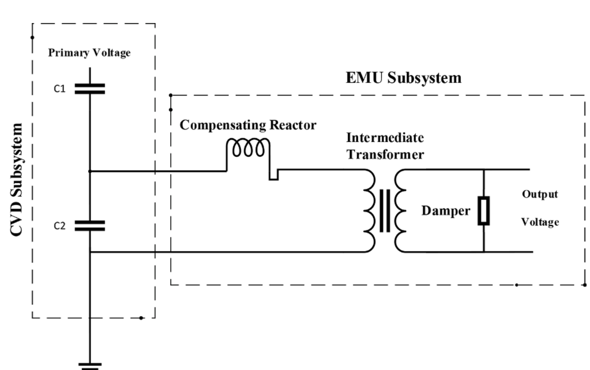

Fig. 1. General circuit structure of a CVT.

Inductive transformers, including windings and cores, have been used to adjust the voltage to an acceptable level for protection and control equipment. It should be noted that the dielectric fluid in the two subsystems of CVT and EMU have their own tanks and are located separately from each other. Fig. 2 shows part of the physical structure of CVT. In this figure, number 1 represents the first capacitor group (C1), number 2 represents the second capacitor group (C2), number 3 represents the EMU subsystem and number 4 indicates the high voltage bushing.

3. The proposed Markov model for evaluating the reliability of CVT

The Markov process relies only on the current state of the system, indicating that what happened to the system in the past has no effect on its future behavior. Therefore, this reliability assessment model is only applied to systems whose behavior involve a lack of memory. This model, which is a sub-branch of the analytical method of reliability assessment, has the potential to predict the future random behavior of the system based on the mathematical relationships and the latest behavioral state of the system [26].

Fig. 3 illustrates the process of modeling and assessing the reliability of CVT. The following steps are considered to obtain the proposed Markov model for CVT.

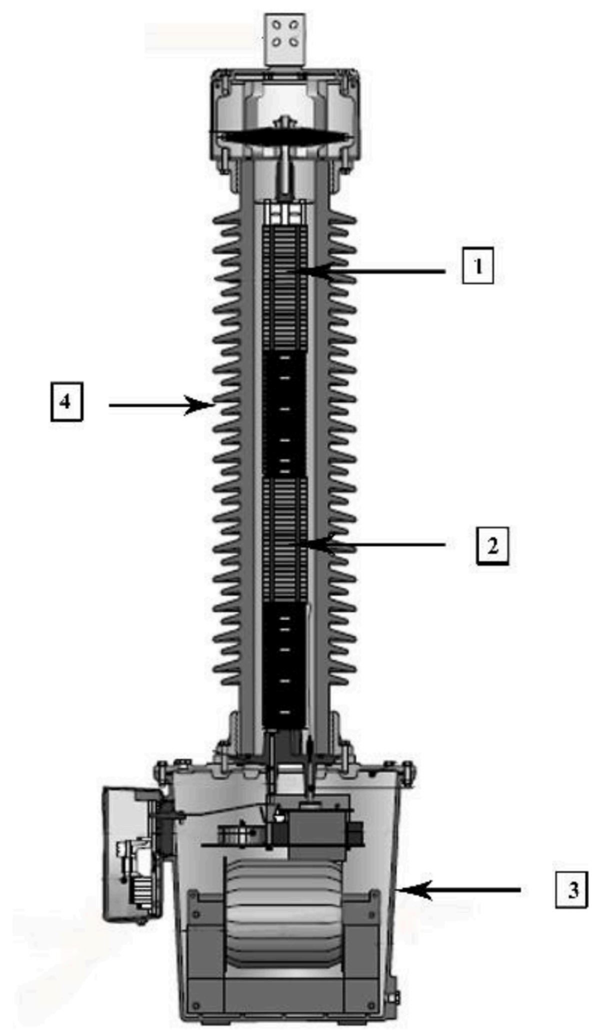

Fig. 2. Physical structure of CVT.

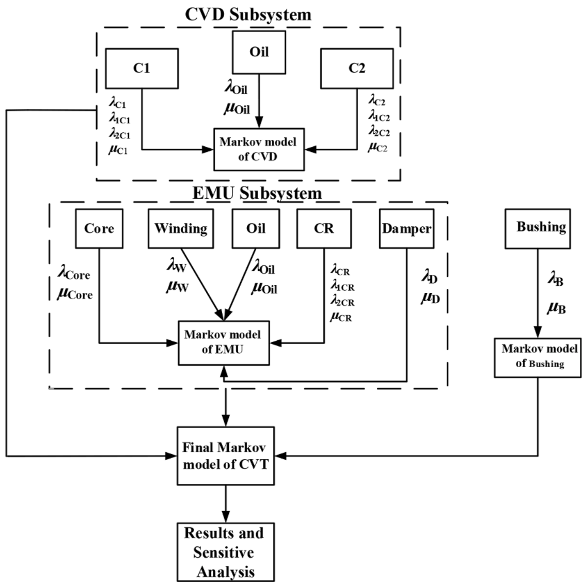

Fig. 3. Process of modeling and assessing of the reliability of CVT.

- CVT is divided into 3 subsystems including CVD, EMU, and high voltage bushing.
- A Markov model is proposed for the CVD subsystem by integrating Markov models of capacitor groups C1 and C2, and dielectric fluid.
- A Markov model is proposed for the EMU subsystem by integrating Markov models of core, winding, compensating reactor, damper, and dielectric fluid.
- A Markov model is presented for the high voltage bushing subsystem.
- Finally, a Markov model is proposed for CVT by integrating the mentioned models.

In this paper, it is assumed that when the failure of an element results in the failure of CVT, the other components will not fail until the CVT is fully restored. It should be noted that, the capacitor groups of C1 and C2 in the CVD subsystem as well as the compensating reactor in the EMU subsystem can make an error that reduces the output accuracy of the CVT, which in this study is considered as low-quality performance, but the other components operate in both healthy and faulty states.

3.1. *The proposed Markov model for CVD*

As mentioned in Section 2, the CVD subsystem consists of two groups of capacitors called C1 and C2, each of which contains a number of series capacitors. These capacitors are completely immersed in fluid. According to the standard [27], the acceptable voltage range of the CVT output can vary in the range of −5 to 10% of the secondary rated voltage. This voltage range is an indication of the low quality state of the CVD unit. This may be due to one of the following two problems:

- One or more series capacitors in the first or second groups have a problem [28].
- The proportionality of the conversion ratio between the first and the second capacitor groups is lost [25].

Therefore, the capacitor groups have three states: healthy, failure and low-quality. Fig. 4 shows the Markov model of the first capacitor group. According to this figure, state 1 corresponds to when the capacitor group C1 is healthy. State 2 occurs when capacitor group C1 fails and causes the capacitor group to go out of circuit. State 3 indicates that one or more series capacitors of the capacitor group C1 are out of circuit, which does not cause the capacitor group to fail, but the output voltage accuracy declines which means that the capacitor group enters

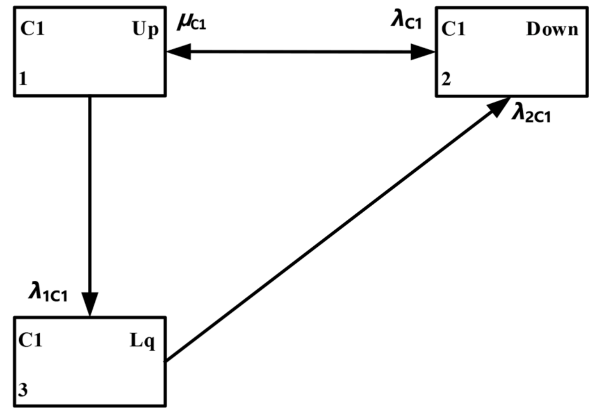

Fig. 4. Markov model for the capacitor group C1 of CVD subsystem.

the low-quality state. Since the number of series capacitors in the first and second groups of capacitors are different, a separate Markov model for the capacitor group C2 is considered which is shown in Fig. 5. Dielectric fluid has two states, healthy and faulty, which in terms of reliability are placed in series with the capacitor groups whose Markov model is shown in Fig. 6. Finally, based on the rules of frequency and continuity of states, a final 10-state Markov model is proposed for the CVD subsystem as shown in Fig. 7.

In the proposed Markov model in Fig. 7, state A1 indicates the healthy performance of the system. That is, the CVT secondary voltage range is within the standard range and the CVT is in the normal range. If there is a change in the conversion ratio of capacitor groups C1 and C2 or an error in the series capacitors of these groups so that the CVT output is out of the normal state but still in the standard range, the model is transferred in B1 and C1 states, respectively, which are considered as low-quality states. If the CVD subsystem fluid fails, the model switches from A1 to E1. If an error occurs in the capacitor groups C1 and C2 so that the conversion ratio is affected or more series capacitors run into problems resulting in deviation in the secondary voltage from the normal state and the standard range, the model enters the D1 and F1 modes, respectively. States D1, E1, and F1, along with each of states G1, H1, I1, and L1, indicate failure of the CVD subsystem. By merging similar modes and based on the rules of frequency and continuity of states, the final 3-state model of Fig. 8 is obtained for the CVD subsystem.

To calculate the reliability assessment, the probabilities of the states in Fig. 7 must be calculated. The probabilities of the states ($\boldsymbol{P}_{\mathrm{CVD}}$) are calculated using (1) [29]. In this relation, $\boldsymbol{A}_{\mathrm{CVD}}$ is a transition matrix defined by (2). In (2), $b_{\mathrm{CVD}ij}$ is the transition rate from state i to state j.

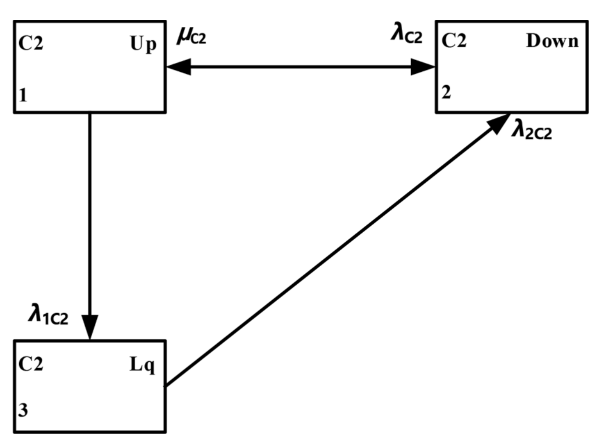

Fig. 5. Markov model for the capacitor group C2 of CVD subsystem.

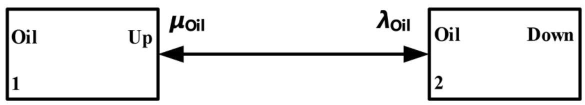

Fig. 6. Markov model of the dielectric fluid for CVD subsystem.

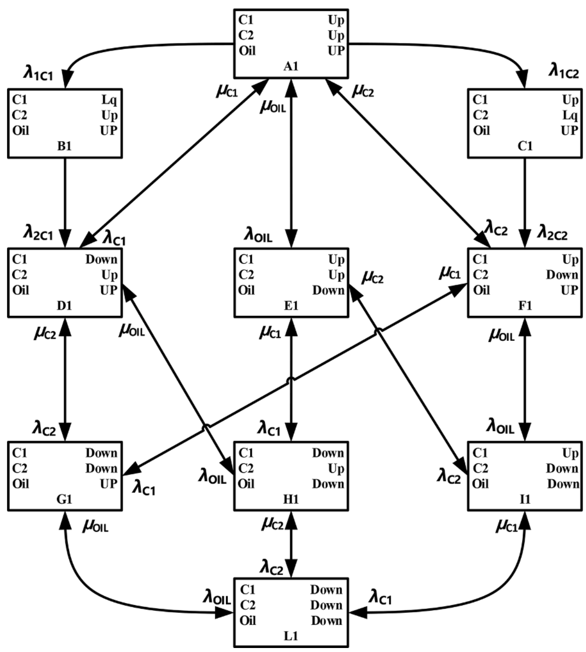

Fig. 7. Proposed extended Markov model for CVD subsystem.

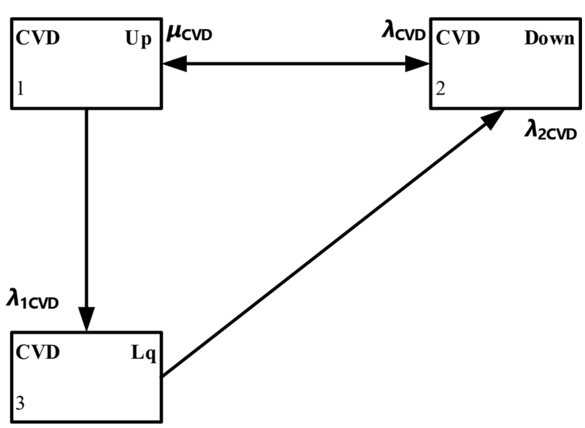

Fig. 8. Equivalent Markov model for CVD subsystem.

$$P_{\mathbf{CVD}} = P_{\mathbf{CVD}} A_{\mathbf{CVD}} \qquad P_{\mathbf{CVD}} = [P_{A1}, P_{B1}, P_{C1}, \cdots\cdots, P_{H1}, P_{I1}, P_{L1}] \tag{1}$$

$$\boldsymbol{A}_{\mathbf{CVD}} = \begin{cases} A_{\mathrm{CVD}ij} = b_{\mathrm{CVD}ij} & i = \mathrm{A1}, \mathrm{B1}, \ldots\ldots, \mathrm{L1} \\ A_{\mathrm{CVD}ii} = 1 - \sum\limits_{j, j \neq i} b_{\mathrm{CVD}ij} & j = \mathrm{A1}, \mathrm{B1}, \ldots\ldots, \mathrm{L1} \end{cases} \tag{2}$$

Since the equation set of (1) is linearly dependent, it is necessary to have an auxiliary Eq. (3) to solve it.

$$\sum_i P_{\mathrm{CVD}i} = 1 \tag{3}$$

Where, $P_{\mathrm{CVD}i}$ is the probability of i^{th} state of CVD extended Markov model, which shows that the sum of the probabilities of the constituent states of the model is one.

The probabilities of the Markov model states corresponding to the CVD subsystem can be calculated according to Fig. 8 using (4) to (6).

$$P_{1\mathrm{CVD}} = P_{\mathrm{A1}} \tag{4}$$

$$P_{2\mathrm{CVD}} = P_{\mathrm{D1}} + P_{\mathrm{E1}} + P_{\mathrm{F1}} + P_{\mathrm{G1}} + P_{\mathrm{H1}} + P_{\mathrm{I1}} + P_{\mathrm{L1}} \tag{5}$$

$$P_{3\mathrm{CVD}} = P_{\mathrm{B1}} + P_{\mathrm{C1}} \tag{6}$$

where, P_{A1} to P_{L1} the probability of occurrence of states A1 to L1 in the Markov model of Fig. 7 and $P_{1\mathrm{CVD}}$, $P_{2\mathrm{CVD}}$ and $P_{3\mathrm{CVD}}$ are the probabilities of healthy, faulty, and low-quality operating states of the CVD subsystem as shown in Fig. 8, respectively.

Eqs. (7) to (10) are used to calculate corresponding failure and repair rates in the model in Fig. 8.

$$\begin{aligned} \lambda_{\mathrm{CVD}} &= \frac{f_{12\mathrm{CVD}}}{P_{1\mathrm{CVD}}} = \frac{f_{\mathrm{A1D1}} + f_{\mathrm{A1E1}} + f_{\mathrm{A1F1}}}{P_{\mathrm{A1}}} = \frac{\lambda_{\mathrm{C1}} P_{\mathrm{A1}} + \lambda_{\mathrm{C2}} P_{\mathrm{A1}} + \lambda_{\mathrm{Oil}} P_{\mathrm{A1}}}{P_{\mathrm{A1}}} \\ &= \lambda_{\mathrm{C1}} + \lambda_{\mathrm{C2}} + \lambda_{\mathrm{Oil}} \end{aligned} \tag{7}$$

$$\lambda_{1\mathrm{CVD}} = \frac{f_{13\mathrm{CVD}}}{P_{1\mathrm{CVD}}} = \frac{f_{\mathrm{A1B1}} + f_{\mathrm{A1C1}}}{P_{\mathrm{A1}}} = \frac{\lambda_{1\mathrm{C1}} P_{\mathrm{A1}} + \lambda_{1\mathrm{C2}} P_{\mathrm{A1}}}{P_{\mathrm{A1}}} = \lambda_{1\mathrm{C1}} + \lambda_{1\mathrm{C2}} \tag{8}$$

$$\lambda_{2\mathrm{CVD}} = \frac{f_{32\mathrm{CVD}}}{P_{3\mathrm{CVD}}} = \frac{f_{\mathrm{B1D1}} + f_{\mathrm{C1F1}}}{P_{\mathrm{B1}} + P_{\mathrm{C1}}} = \frac{\lambda_{2\mathrm{C1}} P_{\mathrm{B1}} + \lambda_{2\mathrm{C2}} P_{\mathrm{C1}}}{P_{\mathrm{B1}} + P_{\mathrm{C1}}} \tag{9}$$

$$\begin{aligned} \mu_{\mathrm{CVD}} &= \frac{f_{21\mathrm{CVD}}}{P_{2\mathrm{CVD}}} = \frac{f_{\mathrm{D1A1}} + f_{\mathrm{E1A1}} + f_{\mathrm{F1A1}}}{P_2} \\ &= \frac{\mu_{\mathrm{C1}} P_{\mathrm{D1}} + \mu_{\mathrm{Oil}} P_{\mathrm{E1}} + \mu_{\mathrm{C2}} P_{\mathrm{F1}}}{P_{\mathrm{D1}} + P_{\mathrm{E1}} + P_{\mathrm{F1}} + P_{\mathrm{G1}} + P_{\mathrm{H1}} + P_{\mathrm{I1}} + P_{\mathrm{L1}}} \end{aligned} \tag{10}$$

3.2. The proposed Markov model for EMU

EMU subsystem includes compensating reactor, middle winding, core, damper and dielectric fluid. The compensating reactor, located in series between the CVD subsystem and the middle winding, is to neutralize the capacitor effects caused by the CVD subsystem. The proposed Markov model of the compensating reactor is illustrated in Fig. 9. Since this component is in series in the circuit, its failure can directly cause the CVT to fail or a failure may occur that reduces the quality of the CVT output. Therefore, this component can have three functional states: healthy, failure and low-quality. The middle winding, the core and the dielectric fluid have a similar function, so that the failure of each of them will cause the CVT to fail. As shown in Fig. 10, these three components can be modeled in terms of reliability in series with two operating states of healthy and faulty.

Eqs. (11) and (12) are defined to determine the corresponding reliability parameters of this set. In these relationships, λ_{Owd} and μ_{Owd} are

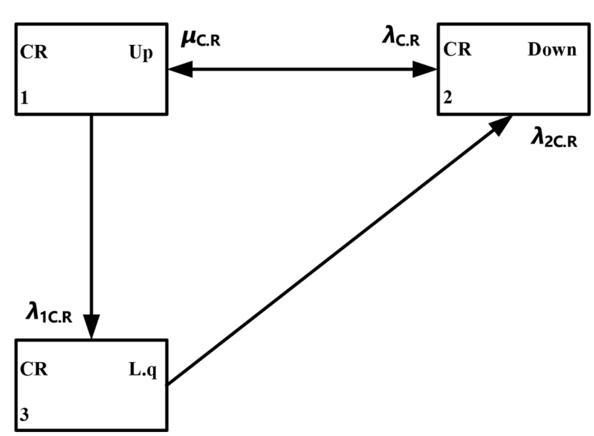

Fig. 9. Markov model for the compensating reactor of EMU subsystem.

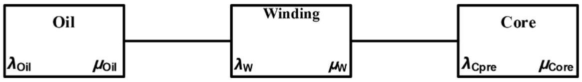

Fig. 10. Markov model for the winding, the core and the dielectric fluid of EMU subsystem.

the failure and repair rates corresponding to the fluid, winding and core components in the EMU subsystem, respectively.

$$\lambda_{Owd} = \lambda_{Oil} + \lambda_W + \lambda_{Core} \tag{11}$$

$$\mu_{Owd} = (\lambda_{Oil} + \lambda_W + \lambda_{Core}) * \left(\frac{\lambda_{Oil}}{\mu_{Oil}} + \frac{\lambda_W}{\mu_W} + \frac{\lambda_{Core}}{\mu_{Core}}\right)^{-1} \tag{12}$$

Finally, the damper is as an open connection in CVT normal operation, and when a fault such as ferroresonance occurs in the network, it protects the equipment fed by CVT, which are mainly protection relays, by a short circuit. Since failure of the damper does not interfere with the normal operation of the CVT, the two operating states of healthy and faulty are considered in accordance with Fig. 11. It should be noted that their faulty performance affects the low-quality state of the EMU subsystem. Fig. 12 shows the proposed Markov model for the electromagnetic unit.

In Fig. 12, the state of A2 represents the healthy operating state of the EMU subsystem. If the damper or CVT internal protection component fails, the model switches from A2 to B2. The model switches from A2 to C2 state when the compensating reactor experiences failure but does not completely goes out of circuit. States B2 and C2 are considered as low-quality states of the EMU subsystem. With the failure of each component of the fluid, the core, the winding, the model switches to state D2 and in case of open connection of the compensating reactor due to an error, the model enters state E2. States D2 and E2 result in failure of the electromagnetic subsystem. In case of a failure in one of the components of the fluid, core and winding, the model shifts from state B2 to F2. The model switches from D2 to G2 state when the compensating reactor fails. With the damper malfunctioning, the model switches from E2 to H2 state. Finally, state I2 indicates a complete failure of the EMU subsystem.

By integrating the similar states, the equivalent Markov model of EMU subsystem is obtained which is shown in Fig. 13.

The probabilities of the EMU subsystem states and its transition matrix are obtained by using (13) and (14), respectively. In (13), $\boldsymbol{P}_{\mathbf{EMU}}$ is the probability of states based on Fig. 12 and in (14), $b_{\mathrm{EMU}ij}$ is the transition rate from state i to state j of the $\boldsymbol{A}_{\mathbf{EMU}}$ transition matrix.

$$\begin{gathered} P_{\mathbf{EMU}} = P_{\mathbf{EMU}} A_{\mathbf{EMU}} \\ P_{\mathbf{EMU}} = [P_{A2}, P_{B2}, P_{C2}, \cdots\cdots\cdots, P_{H2}, P_{I2}] \end{gathered} \tag{13}$$

$$\boldsymbol{A}_{\mathbf{EMU}} = \begin{cases} A_{\mathrm{EMU}ij} = b_{\mathrm{EMU}ij} & i = \mathrm{A2}, \mathrm{B2}, \ldots\ldots, \mathrm{I2} \\ A_{\mathrm{EMU}ii} = 1 - \sum\limits_{j, j \neq i} b_{\mathrm{EMU}ij} & j = \mathrm{A2}, \mathrm{B2}, \ldots\ldots, \mathrm{I2} \end{cases} \tag{14}$$

It is worth noting that, due to the linear dependence of the set of Eqs. (13), an auxiliary equation is needed to solve it, which is shown in (15).

$$\sum_i P_{\mathrm{EMU}i} = 1 \tag{15}$$

As shown in (15), the sum of the probabilities of the $\boldsymbol{P}_{\mathbf{EMU}}$ equals one. Therefore, the probability of the equivalent model states to the EMU subsystem can be calculated according to Fig. 13 using (16) to (18).

$$P_{1\mathrm{EMU}} = P_{A2} \tag{16}$$

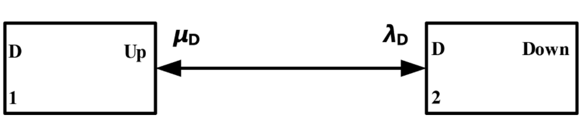

Fig. 11. Markov model for the damper of EMU subsystem.

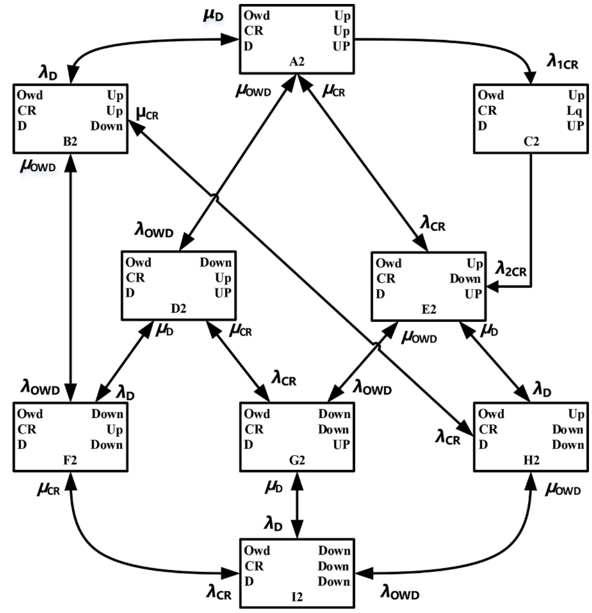

Fig. 12. Proposed extended Markov model for EMU subsystem.

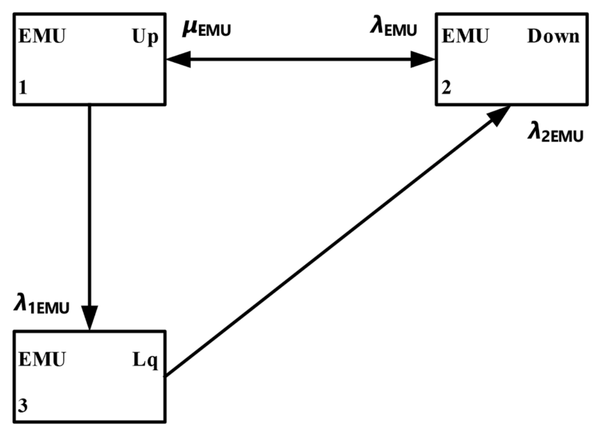

Fig. 13. Equivalent Markov model for EMU subsystem.

$$P_{2\mathrm{EMU}} = P_{D2} + P_{E2} + P_{F2} + P_{G2} + P_{H2} + P_{I2} \tag{17}$$

$$P_{3\mathrm{EMU}} = P_{B2} + P_{C2} \tag{18}$$

where, P_{A2} to P_{I2} are the probabilities of A2 to I2 states in the Markov model of Fig. 12 and $P_{1\mathrm{EMU}}$, $P_{2\mathrm{EMU}}$ and $P_{3\mathrm{EMU}}$ represent the probabilities of healthy, failure and low-quality operating states of the EMU subsystem as shown in Fig. 13, respectively.

Eqs. (19) to (22) are provided for calculating the failure rates and equivalent repairs of the EMU subsystem as shown in Fig. 13.

$$\lambda_{\mathrm{EMU}} = \frac{f_{12\mathrm{EMU}}}{P_{1\mathrm{EMU}}} = \frac{f_{A2D2} + f_{A2E2}}{P_{A2}} = \frac{\lambda_{Owd} P_{A2} + \lambda_{CR} P_{A2}}{P_{A2}} = \lambda_{Owd} + \lambda_{CR} \tag{19}$$

$$\lambda_{1\mathrm{EMU}} = \frac{f_{13\mathrm{EMU}}}{P_{1\mathrm{EMU}}} = \frac{f_{A2B2} + f_{A2C2}}{P_{A2}} = \frac{\lambda_D P_{A2} + \lambda_{1CR} P_{A2}}{P_{A2}} = \lambda_D + \lambda_{1CR} \tag{20}$$

$$\lambda_{2\mathrm{EMU}} = \frac{f_{32\mathrm{EMU}}}{P_{3\mathrm{EMU}}} = \frac{f_{C2E2} + f_{B2F2}}{P_{B2} + P_{C2}} = \frac{\lambda_{Owd} P_{B2} + \lambda_{2CR} P_{C2}}{P_{B2} + P_{C2}} \tag{21}$$

$$\mu_{\mathrm{EMU}} = \frac{f_{21\mathrm{EMU}}}{P_{2\mathrm{EMU}}} = \frac{f_{D2A2} + f_{E2A2}}{P_{2\mathrm{EMU}}} = \frac{\mu_{Owd} P_{D2} + \mu_{CR} P_{E2}}{P_{D2} + P_{E2} + P_{F2} + P_{G2} + P_{H2} + P_{I2}} \tag{22}$$

3.3. The final proposed Markov model of the CVT

In this section, to determine the proposed Markov model of the CVT, the Markov model of CVD and EMU subsystems are integrated, and the Markov high voltage bushing model will be added to them. Since failure of the high voltage bushing can cause CVT to fail, two healthy and faulty states can be considered for bushing. Fig. 14 depicts the two- state Markov model of bushing.

Next, by integrating the three subsystems related to CVT, its extended Markov model is proposed according to Fig. 15. In this model, direct failure of any subsystem of the CVD, EMU, and bushing can cause the CVT to fail, which corresponds to states D3, F3, and E3, respectively. States B3 and C3 are low-quality states that may occur when a failure occurs in the CVD and EMU subsystems, respectively, while the CVT continues to operate at an acceptable quality drop in output voltage. In the event of a failure of the CVD subsystem or the EMU subsystem that results in CVT failure, the Markov model switches from A3 to D3 and F3 states, respectively. In case of failure in the high voltage bushing, the model changes from A3 state to E3 state. In case of a failure in the CVD subsystem, the model shifts from F3 to I3 state. When the EMU subsystem fails, the model moves from E3 to H3 state. When the high voltage bushing fails, the model moves from D3 to G3 state. In this model, L3 state represents complete failure of CVT. With the occurrence of each of the states D3, E3, F3 or G3, H3, I3 and L3, the CVT will fail and go out of circuit. Fig. 16 shows the equivalent Markov model of a CVT, which consists of three states: healthy, failure, and low-quality performance.

The probability of each of the states in Fig. 15 comes from (23), and (24) is used to construct the transition matrix $\boldsymbol{A}_{\mathbf{CVT}}$ of the extended Markov CVT model in accordance with Fig. 15. $\boldsymbol{P}_{\mathbf{CVT}}$ is the probability of states and $b_{\mathrm{CVT}ij}$ is the rate of transition from state i to state j.

$$\begin{gathered} P_{\mathbf{CVT}} = P_{\mathbf{CVT}} A_{\mathbf{CVT}} \\ P_{\mathbf{CVT}} = [P_{\mathrm{A3}}, P_{\mathrm{B3}}, P_{\mathrm{C3}}, \cdots\cdots\cdots, P_{\mathrm{H3}}, P_{\mathrm{I3}}, P_{\mathrm{L3}}] \end{gathered} \tag{23}$$

$$A_{\mathbf{CVT}} = \begin{cases} A_{\mathrm{CVT}ij} = b_{\mathrm{CVT}ij} & i = \mathrm{A3}, \mathrm{B3}, \ldots\ldots, \mathrm{L3} \\ A_{\mathrm{CVT}ii} = 1 - \sum\limits_{j, j \neq i} b_{\mathrm{CVT}ij} & j = \mathrm{A3}, \mathrm{B3}, \ldots\ldots, \mathrm{L3} \end{cases} \tag{24}$$

An auxiliary Eq. (25) is needed to solve 23.

$$\sum_i P_{\mathrm{CVT}i} = 1 \tag{25}$$

The probability of occurrence of any of the equivalent Markov states of CVT can be calculated using (26) to (28) according to the extended Markov model for CVT shown in Fig. 15.

$$P_{1\mathrm{CVT}} = P_{\mathrm{A3}} \tag{26}$$

$$P_{2\mathrm{CVT}} = P_{\mathrm{D3}} + P_{\mathrm{E3}} + P_{\mathrm{F3}} + P_{\mathrm{G3}} + P_{\mathrm{H3}} + P_{\mathrm{I3}} + P_{\mathrm{L3}} \tag{27}$$

$$P_{3\mathrm{CVT}} = P_{\mathrm{B3}} + P_{\mathrm{C3}} \tag{28}$$

In brief, equivalent rates of CVD subsystem (λ_{CVD}, $\lambda_{1\mathrm{CVD}}$, $\lambda_{2\mathrm{CVD}}$ and μ_{CVD}) are obtained according to Figs. 7 and 8. Moreover, the equivalent rates of EMU subsystem (λ_{EMU}, $\lambda_{1\mathrm{EMU}}$, $\lambda_{2\mathrm{EMU}}$ and μ_{EMU}) are obtained based on Figs. 12 and 13. By using the obtained equivalent rates, the rates of high voltage bushing (λ_{B} and μ_{B}) and combining the same states as Fig. 15, the equivalent rates of CVT (λ_{CVT}, $\lambda_{1\mathrm{CVT}}$, $\lambda_{2\mathrm{CVT}}$ and μ_{CVT}) are obtained based on Fig. 16 for evaluating the reliability of CVT. Eqs. (29) to (32) are defined for calculating the equivalent rates of CVT.

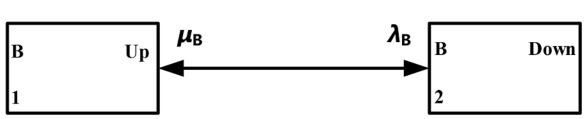

Fig. 14. Markov model for high voltage bushing subsystem.

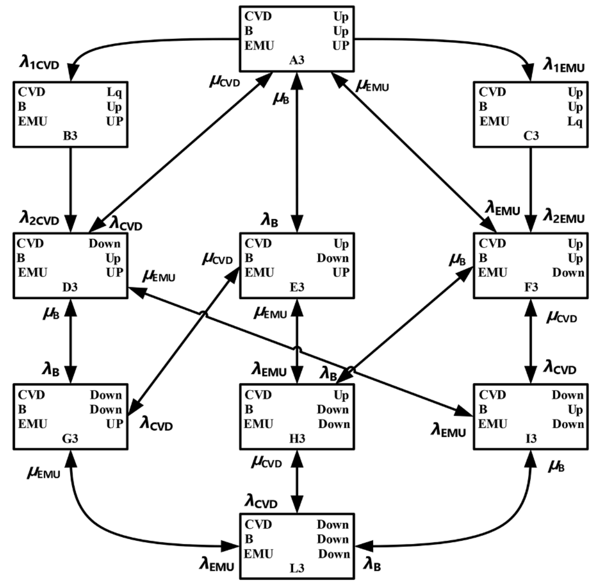

Fig. 15. Proposed extended Markov model for CVT.

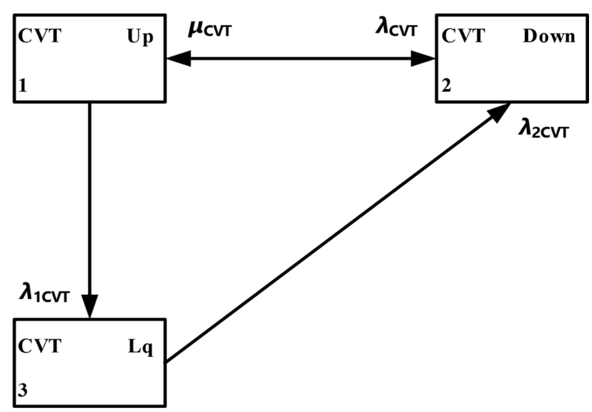

Fig. 16. Equivalent Markov model for CVT.

$$\begin{aligned} \lambda_{\mathrm{CVT}} &= \frac{f_{12\mathrm{CVT}}}{P_{1\mathrm{CVT}}} = \frac{f_{\mathrm{A3D3}} + f_{\mathrm{A3E3}} + f_{\mathrm{A3F3}}}{P_{\mathrm{A3}}} = \frac{\lambda_{\mathrm{CVD}} P_{\mathrm{A3}} + \lambda_{\mathrm{B}} P_{\mathrm{A3}} + \lambda_{\mathrm{EMU}} P_{\mathrm{A3}}}{P_{\mathrm{A3}}} \\ &= \lambda_{\mathrm{CVD}} + \lambda_{\mathrm{B}} + \lambda_{\mathrm{EMU}} \end{aligned} \tag{29}$$

$$\lambda_{1\mathrm{CVT}} = \frac{f_{13\mathrm{CVT}}}{P_{1\mathrm{CVT}}} = \frac{f_{\mathrm{A3B3}} + f_{\mathrm{A3C3}}}{P_{\mathrm{A3}}} = \frac{\lambda_{1\mathrm{CVD}} P_{\mathrm{A3}} + \lambda_{1\mathrm{EMU}} P_{\mathrm{A3}}}{P_{\mathrm{A3}}} = \lambda_{1\mathrm{CVD}} + \lambda_{1\mathrm{EMU}} \tag{30}$$

$$\lambda_{2\mathrm{CVT}} = \frac{f_{32\mathrm{CVT}}}{P_{3\mathrm{CVT}}} = \frac{f_{\mathrm{B3D3}} + f_{\mathrm{C3F3}}}{P_{\mathrm{B3}} + P_{\mathrm{C3}}} = \frac{\lambda_{2\mathrm{CVD}} P_{\mathrm{B3}} + \lambda_{2\mathrm{EMU}} P_{\mathrm{C3}}}{P_{\mathrm{B3}} + P_{\mathrm{C3}}} \tag{31}$$

$$\begin{aligned} \mu_{\mathrm{CVT}} &= \frac{f_{21\mathrm{CVT}}}{P_{2\mathrm{CVT}}} = \frac{f_{\mathrm{D3A3}} + f_{\mathrm{E3A3}} + f_{\mathrm{F3A3}}}{P_{2\mathrm{CVT}}} \\ &= \frac{\mu_{\mathrm{CVD}} P_{\mathrm{D3}} + \mu_{\mathrm{B}} P_{\mathrm{E3}} + \mu_{\mathrm{EMU}} P_{\mathrm{F3}}}{P_{\mathrm{D3}} + P_{\mathrm{E3}} + P_{\mathrm{F3}} + P_{\mathrm{G3}} + P_{\mathrm{H3}} + P_{\mathrm{I3}} + P_{\mathrm{L3}}} \end{aligned} \tag{32}$$

4. Simulation results

In order to investigate the performance of the proposed Markov model in evaluating the reliability of the CVT, initially, its reliability is calculated in a basic state. Then, the sensitivity analysis is carried out to analyze the effect of CVT components failure rate on its reliability.

4.1. Basic state

In this section, to evaluate the reliability of CVT, the input parameters of the Markov model, including failure and repair rates and of all CVT components, are considered in accordance Table 1. The calculated failure and repair rates for the Markov models of the various subsystems and the final CVT model are shown in Table 2. Using the calculated input parameters, the switching frequency of the different states for each of the CVT subsystems is calculated, as shown in this table.

Table 3 provides the probabilities of the CVT operating states shown in Fig. 16. The results of this table indicate that the maximum operating time of a CVT in a healthy state with appropriate measurement quality, has a probability of 0.91145225. The results also indicate that the probability of CVT failure when the output of the secondary voltage is out of the standard range is equal to 0.00046703. The presented results of a practical study in [23] show that the probability of CVT failure is equal to 0.000539. Comparison of these results indicates the efficiency of the proposed Markov model for evaluating the reliability of capacitive voltage transformers.

4.2. The effect of CVT components failure rate on its reliability

To carry out the sensitivity analysis, the reliability of the CVT is evaluated by varying the failure rate of different components of each subsystem of the CVT. In the following, as an example, the effect of failure rate of capacitor group C2, compensating reactor, damper and bushing on the reliability of CVT is presented.

In this regard, by changing the failure rate of the second capacitor group of the CVD subsystem, from the basic state (0.00602) in the form of increasing and decreasing steps with step of 0.00602, the rate of change of the probability of occurrence of healthy, failure and low-quality states of CVT is calculated. The simulation results are shown in Table 4. The results indicate that with increasing the failure rate of the second capacitor group, the probability of CVT in healthy and low-quality states decreases, and the probability of failure CVT increases. For example, by increasing the failure rate of the capacitor group C2 subsystem from 0.00602 to 0.02408, the probability of healthy state decreases from 0.91145225 to 0.91109953, the probability of low-quality state decreases from 0.08808071 to 0.08804662 and the probability failure state increases from 0.00046703 to 0.00085383.

Table 1
Failure and repair rates data.

Failure rate	Value (f/yr)
λ_{C1}	0.000463
λ_{1C1}	0.0000463
λ_{2C1}	0.0004167
λ_{C2}	0.00602
λ_{1C2}	0.000602
λ_{2C2}	0.005418
λ_{Oil}	0.003
λ_{Core}	0.0005
λ_{W}	0.0045
λ_{CR}	0.0152550
λ_{1CR}	0.0005
λ_{2CR}	0.01
λ_{D}	0.0001
λ_{B}	0.003
Repair rate	**Value (r/yr)**
μ_{C1}	100
μ_{C2}	100
μ_{Oil}	23
μ_{Core}	19
μ_{W}	100
μ_{CR}	100
μ_{D}	100
μ_{B}	182.5

Table 2
Obtained failure, repair and frequency rates of Markov models.

Failure rate	Value (f/yr)	Repair rate	Value (r/yr)	Frequency rate	Value (occ/y)
λ_{CVD}	0.0095	μ_{CVD}	74.7230	F_{12CVD}	0.0072
λ_{1CVD}	0.0006483	μ_{OWD}	39.6529	F_{13CVD}	5.3034e10^{-4}
λ_{2CVD}	0.0029	μ_{EMU}	66.1087	F_{21CVD}	0.0123
λ_{OWD}	0.0080	μ_{CVT}	72.1810	F_{32CVD}	5.3032e10^{-4}
λ_{EMU}	0.0233			F_{12EMU}	0.0217
λ_{1EMU}	0.0006			F_{13EMU}	5.7123e10^{-4}
λ_{2EMU}	0.01			F_{21EMU}	0.0226
λ_{CVT}	0.0357			F_{32EMU}	4.7603e10^{-4}
λ_{1CVT}	0.0012				
λ_{2CVT}	0.0129				

Table 3
Probability and frequency of the CVT model states.

Frequency	Value (occ/yr)	Probability	Value
F_{21CVT}	0.0337	P_{1CVT}	0.91145225
F_{12CVT}	0.0314	P_{2CVT}	0.00046703
F_{13CVT}	0.0010	P_{3CVT}	0.08808071
F_{32CVT}	0.0011		

Table 4
Probability of equivalent Markov model for CVT states by change of λ_{C2}.

λ_{C2} (f/yr)	P_{1CVT}	P_{2CVT}	P_{3CVT}
0.001505	0.91151193	0.00040158	0.08808647
0.00301	0.91149376	0.00042151	0.08808472
0.00602	**0.91145225**	**0.00046703**	**0.08808071**
0.01204	0.91135182	0.00057717	0.08807100
0.02408	0.91109953	0.00085383	0.08804662

In the EMU subsystem, the rate of change in the probability of occurrence of healthy, failure and low-quality CVT states is calculated by changing the failure rate of the compensating reactor and damper. In this regard, the failure rate of the reactor changes from the basic state (0.0152550) by increasing and decreasing steps of 0.0152550. The simulation results are shown in Table 5. The results indicate that with increase failure rate of the reactor, the probability of CVT operation in the failure state will significantly increase. The probability failure state of CVT by considering 0.06102 for λ_{CR} is 1.9 times higher than the basic state.

By changing the failure rate of the damper with steps similar to the compensating reactor, probability of equivalent Markov model of CVT states is calculated. As mentioned in Section 3.2, failure mode of damper effects on low-quality state of EMU subsystem and finally CVT, results in Table 6 proves this. By increasing the failure rate of the damper from 0.0001 to 0.0004, the probability of CVT operating in the healthy and failure states decreases from 0.91145225 to 0.89255423 and from 0.00046703 to 0.00046106, respectively. The low-quality state of the CVT increases significantly from 0.08808071 to 0.10698470.

Table 7 depicts the effect of failure rate of high voltage bushing on the probability of CVT operating states. In this study, the failure rate of the high voltage bushing changes from the basic state (0.003) in the form of increasing and decreasing steps with a step of 0.003. The results

Table 5
Probability of equivalent Markov model for CVT states by change of λ_{CR}.

λ_{CR} (f/yr)	P_{1CVT}	P_{2CVT}	P_{3CVT}
0.00381375	0.91154752	0.00036255	0.08808991
0.0076275	0.91151560	0.00039756	0.08808683
0.0152550	**0.91145225**	**0.00046703**	**0.08808071**
0.03051	0.91132585	0.00060564	0.08806849
0.06102	0.91107296	0.00088298	0.08804405

Table 6
Probability of equivalent Markov model for CVT states by change of λ_D.

λ_D (f/yr)	P_{1CVT}	P_{2CVT}	P_{3CVT}
0.000025	0.91630240	0.00046857	0.08322902
0.00005	0.91467996	0.00046805	0.08485197
0.0001	**0.91145225**	**0.00046703**	**0.08808071**
0.0002	0.90506465	0.00046501	0.09447032
0.0004	0.89255423	0.00046106	0.10698470

Table 7
Probability of equivalent Markov model for CVT states by change of λ_B.

λ_B (f/yr)	P_{1CVT}	P_{2CVT}	P_{3CVT}
0.00075	0.91146191	0.00045644	0.08808164
0.0015	0.91145869	0.00045996	0.08808133
0.003	**0.91145225**	**0.00046703**	**0.08808071**
0.006	0.91143926	0.00048127	0.08807945
0.012	0.91141303	0.00051004	0.08807692

indicate that by reducing the failure rate of bushing from 0.003 to 0.00075, the probability of healthy state increases from 0.91145225 to 0.91146191. Also, the probability of faulty state decreases from 0.00046703 to 0.00045644 and the probability of low-quality state increases from 0.08808071 to 0.08808164.

5. Conclusion

Maintaining the quality of output signals from instrument transformers has a vital role in the proper operation of the protection systems. Therefore, evaluation the reliability of the transformers during their lifetime is very important. In this study, a Markov model has been proposed to evaluate the reliability CVT as one of the most important instrument transformers. To achieve the proposed Markov model, initially, a 10-state, a 9-state, and 2-state Markov models have been presented for CVD, EMU, and high voltage bushing as CVT subsystems, respectively. Next, by integrating these models of the subsystems, an extended 10-state model and finally, an equivalent 3-satae model have been proposed for CVT. Based on the obtained results, it can be seen that CVT in more than 90% of its life is in good condition, and with suitable measurement quality. Moreover, the probability of CVT failure has been obtained 0.00046703, which is approximately equal to the presented practical result in [23]. According to the sensitivity analysis, second capacitive group in the CVD subsystem, and the compensating reactor in the EMU subsystem have a significant effect on the reliability of CVT. Based on the presented explanations, the proposed model has the desirable efficiency in evaluating the reliability of CVT.

CRediT authorship contribution statement

Omid Haghgoo: Conceptualization, Methodology, Software, Writing – original draft. **Yaser Damchi:** Conceptualization, Methodology, Writing – review & editing, Supervision.

Declaration of Competing Interest

No conflict interest exists. Funding was not received for this work

References

[1] Z. WU, S. li, Reliability evaluation and sensitivity analysis to AC/UHVDC systems based on sequential Monte Carlo simulation, IEEE Trans. Power Syst. 34 (2019) 3156–3167.
[2] R. Kenarangui, Event-tree analysis by fuzzy probability, IEEE Trans. Reliability 40 (1991) 120–124.
[3] X. Shu, Y. Guo, W. Yang, K. Wei, Y. Zhu, H. Zou, A detailed reliability study of the motor system in pure electric vans by the approach of fault tree analysis, IEEE Access 8 (2020) 5295–5307.
[4] S. Wang, C. Fernandez, C. Yu, Y. Fan, W. Cao, D. Store, A novel charged state prediction method of the lithium ion battery packs based on the composite equivalent modeling and improved splice Kalman filtering algorithm, J. Power Sources (2020) 471. September.
[5] P.M. Anderson, S.K. Agarwal, An improved model for protective-system reliability, IEEE Trans. Reliability 41 (1992) 422–426.
[6] R. Billinton, M. Fotuhi-Firuzabad, T.S. Sidhu, Determination of the optimum routine test and self-checking intervals in protective relaying using a reliability model, IEEE Trans. Power Syst. 17 (2002) 663–669.
[7] Y. Damchi, J. Sadeh, Considering failure probability for back-up relay in determination of the optimum routine test interval in protective system using Markov model, IEEE Power Energy Society Gen. Meeting 2009; 1–5.
[8] Y. Damchi, J. Sadeh, Determination of the optimum routine and self-checking test time intervals for power system protection considering remote back-up protection system failure, IET Generation, Transmission Distribution 7 (2012) 1163–1171.
[9] Y. Damchi, J. Sadeh, Effect of remote back-up protection system failure on the optimum routine test time interval of power system protection, Iranian J. Electr. Electronic Eng. 9 (2013) 237–245.
[10] W.L.Kling J.J.Meeuwsen, Effects of preventive maintenance on circuit breakers and protection systems upon substation reliability, Electr.Power Syst. Res. (1996) 181–188. September.
[11] S. Zhao, X. Yan, B. Wang, E. Wang, L. Ma, Research on reliability evaluation method of DC circuit breaker based on Markov model, Electr. Power Syst. Res. 173 (2019) 1–5.
[12] K. Jiang, C. Singh, New models and concepts for power system reliability evaluation including protection system failures, IEEE Trans. Power Syst. 4 (2011) 1845–1855. November.
[13] A. Karimabadi, M.E. Hajiabadi, E. Kamyab, A.A. Shojaei, Determining the optimal inspection rate of circuit breakers equipped with condition monitoring devices using new maintenance Markov model, Int.Trans. Electr.Energy Syst. 30 (2020) 1–22. April.
[14] H. Farzin, M. Monadi, M. Fotuhi-Firuzabad, M. Savaghebi, A reliability model for overcurrent relays considering harmonic-related malfunctions, Int. J. Electr. Power Energy Syst. 131 (2021). October.
[15] M. Sefidgaran, M. Mirzaie, A. Ebrahimzadeh, Reliability model of power transformer with ONAN cooling, Iranian J. Electr. Electronic Eng. 6 (2010) 103–109.
[16] M. Sefidgaran, M. Mirzaie, A. Ebrahimzadeh, Reliability model of the power transformer with ONAF cooling, Int J Electr Power Energy Syst 35 (2011) 97–104.
[17] A. Karami-Horestani, M.E. Hamedani-Golshan, H. Hajian, Reliability modeling of TCR–FC type SVC using Markov process, Int J Electr Power Energy Syst 55 (2014) 305–311.
[18] M.S. Alvarez-Alvarado, D. Jayaweera, Reliability-based smart-maintenance model for power system generators, IET Generation, Transmission & Distribution 14 (2020) 1770–1780. March.
[19] M. Haghshenas, R. Hooshmand, Modeling and reliability evaluation of magnetically controlled reactor based on the Markov process technique, Iranian J. Electr. Comp. Eng. 17 (2019) 165–176.
[20] A.A. Sallam, M. Desouky, H. Desouky, Shunt capacitor effect on electrical distribution system reliability, IEEE Trans. Reliability 43 (1994) 170–176.
[21] A. Mirsamadi, Y. Damchi, M. Assili, Impact of human error modeling on failure rate and optimum routine test interval of protection system, Iranian J. Electr. Comp. Eng. 17 (2021) 1–9.
[22] D.R. Morais, J.G. Rolim, J. Coser, H.H. Zurn, Reliability centered maintenance for capacitor voltage transformers, 9th International Conference on Probabilistic Methods Applied to Power Systems KTH Stockholm, Sweden 2006; 1–6.
[23] Z. Meng, H. Li, C. Zhang, M. Chen, Q. Chen, Research on the reliability of capacitor voltage transformers calibration results. Measurement, Elsevier, 2019, pp. 770–779, 146.
[24] W. Dong, K. Zha, C. Gao, F. Ji, Z. He, Rated capacitance determination of a new 1000 kV equipotential shielding capacitor voltage transformer under the interference of stray capacitance, IEEE Trans. Power Delivery 33 (2018) 2078–2086.
[25] Oil Insulated Outdoor Instrument Transformers Buyer's Guide. ABB 2012 -09, Edition 7.
[26] R. Billinton, R.N. Allan, Reliability Evaluation of Engineering System, 2nd ed., Plenum, New York, 1994.
[27] IEC Standards 61869-5, Instrument Transformers – Part 5: Additional requirements For Capacitor Voltage Transformers, Edition 1.0, 2011.
[28] Y. Liu, J. Liang, Y. Han, B. Niu, Z. Lu, H. Yang, An analysis and calculation on the problems of CVT caused by capacitor element breakdown, 2nd IEEE Conference on Energy Internet and Energy System Integration (EI2), Beijing 2018; 1–4.
[29] R. Billinton, R.A. Allan, Reliability Evaluation of Power Systems 1996; 400–440.